Antenna Trajectory-Aware Sum-Rate Maximization for Fluid Antenna-Enhanced Wireless Networks

Biqian Feng*, Chenyuan Feng*, Wenchao Xia[†], Chongwen Huang[‡], Hongbo Zhu[†],
Kai-Kit Wong[§], Fellow, IEEE, and Tony Q. S. Quek[¶], Fellow, IEEE

* Department of Communication System, EURECOM, Sophia Antipolis, France

† Wireless Communication Key Laboratory of Jiangsu Province, Nanjing University of Posts and Telecommunications, China

‡ College of Information Science and Electronic Engineering, Zhejiang University, China

§ Department of Electronic and Electrical Engineering, University College London, United Kingdom

¶ Information System and Technology Design Pillar, Singapore University of Technology and Design, Singapore Email: {Biqian.Feng, Chenyuan.Feng}@eurecom.fr, {xiawenchao,zhuhb}@njupt.edu.cn, chongwenhuang@zju.edu.cn, kai-kit.wong@ucl.ac.uk, tonyquek@sutd.edu.sg

Abstract—This paper investigates the non-negligible latency associated with repositioning fluid antennas (FA) and delves into the challenge of maximizing the antenna trajectory-aware sum-rate for FA-enhanced systems. Different with conventional transmission schemes that swiftly reposition antennas to their desired positions, we introduce an innovative protocol that jointly optimizes antenna movement and signal transmission during the repositioning phase. To reduce the computational complexity, we reformulate the problem into a more tractable weighted minimum mean square error (WMMSE) framework, which is particularly tailored for FAs. Subsequently, we employ the WMMSE algorithm and a majorization-minimization technique to refine the beamforming strategies and antenna positioning, respectively. Furthermore, we introduce a planar motion mode that confines each FA within a designated region, leading to a lowcomplexity, closed-form solution. Numerical results demonstrate that the antenna trajectory-aware FA-enhanced system surpasses traditional systems in performance.

Index Terms—Fluid antenna, antenna trajectory, sum rate maximization, planar motion mode.

I. INTRODUCTION

As the antenna technology continues to evolve, multiple-input multiple-output (MIMO) systems have experienced a remarkable expansion in capacity, capitalizing on the additional spatial degrees of freedom (DoFs). Nonetheless, traditional MIMO systems, which rely on fixed-position antennas (FPAs), encounter limitations in achieving further performance improvements. In light of the recent advancements in liquid metal technology, fluid antennas (FAs) have emerged as a cutting-edge solution. These antennas dynamically adapt their physical positioning in response to the time-varying dynamics of wireless channels, thereby optimizing MIMO system capabilities.

A multitude of research efforts have been dedicated to the analysis and enhancement of FA-enhanced MIMO systems. Works such as [4], [5] have explored the deployment of FAs in

This work was supported in part by the National Natural Science Foundation of China under Grant 62301328.

Corresponding author: Chenyuan Feng.

transceivers to bolster the capabilities of point-to-point MIMO systems. Furthermore, studies like [6], [7] have examined multiuser transmission scenario where FAs are exclusively integrated into the base station (BS). Specifically, the motions of the FA elements, constrained by practical device performance, has been conceptualized as discrete actions, referred to as ports. Additionally, [8] has investigated scenarios where only users are equipped with FAs. Moreover, drawing on the potential of FAs, a spectrum of recent research has delved into optimizing their performance under diverse configurations, including physical-layer security [9], integrated sensing and communication (ISAC) [10], over-the-air computation [11], and mobile edge computing [12], among others. However, the antenna adjustment often introduces non-negligible delays, which can substantially impact system performance [13]. Particularly, the adjustment of one antenna may be subject to constraints imposed by the positions of adjacent antennas to avoid collisions or mutual coupling, further intensifying the actuation delay. Consequently, such delays can degrade the effective data transmission rate, especially when the channel coherence time is limited.

Hence, this paper aims to investigate the FA trajectoryaware sum-rate maximization problem. The main contributions of this paper are summarized as follows: i) We first develop an FA trajectory-aware sum-rate maximization problem, which is subsequently transformed into an equivalent weighted minimum mean square error (WMMSE) problem compatible with FAS, thereby significantly improving the problem's tractability. ii) To solve this problem efficiently, we employ the block coordinate descent (BCD) method to iteratively optimize all variables and adopt a planar motion mode to derive a low-complexity closed-form solution for FA trajectory. iii) Numerical results demonstrate that the FAenhanced systems outperform their traditional counterparts. Moreover, the adoption of the planar motion mode notably decreases computational demands, albeit with a minor tradeoff in performance.

II. SYSTEM MODEL

We consider a multi-user downlink FA-enhanced system, which consists of a BS equipped with M FAs and K single-FA users. Unlike conventional systems, this setup allows the positions of transmit FA at Bs and the receive FA at user k to be dynamically adjusted within \mathcal{C}^t and \mathcal{C}^r_k respectively. This flexibility, enabled by technologies such as liquid metal [1], [2], enhances spatial diversity gains. Instead of following traditional transmission protocols, which rapidly reposition antennas to target locations but experience reduced transmission rates during adjustments, we introduce an innovative approach to simultaneously optimize antenna trajectory and signal transmission over multiple time slots.

Let S denote the number of time slots within the channel coherence time, with each slot having a duration of τ . The position of FA m at the BS and that of the FA for user k during the s-th time slot are given by $\mathbf{t}_m(s) = (x_m(s), y_m(s))^T$ and $\mathbf{r}_k(s) = (x_k(s), y_k(s))^T$, respectively. Hence, during s-th time slot, the position vector of all transmit FAs at BS and receive FA at users can be expressed as $\mathbf{t}(s) = (\mathbf{t}_1(s)^T, \cdots, \mathbf{t}_M(s)^T)^T$ and $\mathbf{r}(s) = (\mathbf{r}_1(s)^T, \cdots, \mathbf{r}_K(s)^T)^T$, respectively. To ensure practical feasibility and enhance antenna efficiency, a minimum inter-FA distance of D is maintained between any two FAs at the BS to mitigate potential electrical coupling, i.e.,

$$\|\mathbf{t}_i(s) - \mathbf{t}_j(s)\| \ge D, \forall i \ne j, \forall s.$$
 (1)

Due to the limited power available to operate the FAs, a maximum allowable speed is imposed on each FA, i.e.,

$$\|\mathbf{t}_{m}(s) - \mathbf{t}_{m}(s-1)\| \le V_{\max}^{t} \tau, \forall m, \forall s, \|\mathbf{r}_{k}(s) - \mathbf{r}_{k}(s-1)\| \le V_{\max}^{r} \tau, \forall k, \forall s,$$
(2)

where V_{\max}^t and V_{\max}^r represent the maximum speeds of each FA at the BS and the users, respectively. $\mathbf{t}_m(0)$ and $\mathbf{r}_k(0)$ denote the initial positions of the transmit FA m at the BS and the receive FA for user k before adjustment, respectively.

In an FA-enhanced system, the channel response for user k is influenced by the position vector that can be expressed as $\mathbf{h}_k(\mathbf{t}(s), \mathbf{r}_k(s)) \in \mathbb{C}^{M \times 1}$ during the s-th time slot. Thus, the received signal is given by

$$y_k(s) = \mathbf{h}_k^H(\mathbf{t}(s), \mathbf{r}_k(s)) \sum_{k=1}^K \mathbf{w}_k(s) s_k(s) + z_k(s), \quad (3)$$

where $\mathbf{w}_k(s) \in \mathbb{C}^{M \times 1}$ and $s_k(s) \in \mathbb{C}$ represent the beamforming vector and the transmit signal intended for user k, respectively. By combining all beamformers, the beamforming matrix is defined as $\mathbf{W}(s) \triangleq (\mathbf{w}_1(s), \mathbf{w}_2(s), \cdots, \mathbf{w}_K(s)) \in \mathbb{C}^{M \times K}$. The term $z_k(s) \sim \mathcal{CN}(0, \sigma^2)$ represents the additive noise. Furthermore, the signal-to-interference-plus-noise ratio (SINR) at user k can be expressed as

$$\gamma_k(s) \triangleq \frac{|\mathbf{h}_k^H(\mathbf{t}(s), \mathbf{r}_k(s))\mathbf{w}_k(s)|^2}{\sum\limits_{s \neq k} |\mathbf{h}_k^H(\mathbf{t}(s), \mathbf{r}_k(s))\mathbf{w}_i(s)|^2 + \sigma^2}.$$
 (4)

A. Channel Model based on Field-Response

At time s, the difference of the signal propagation distance for the l-th AoD of user k between the FA m position and the origin at the BS is measured as

$$\rho_{l,k}^{t}(\mathbf{t}_{m}(s)) = x_{m}(s)\sin\theta_{l,k}^{t}\cos\phi_{l,k}^{t} + y_{m}(s)\cos\theta_{l,k}^{t},$$
(5)

where $(\theta_{l,k}^t, \phi_{l,k}^t)$ denotes the elevation and azimuth AoDs for the l-th transmit paths between the BS and user k. Similarly, the signal propagation phase difference for the l-th AoA between the FA and the reference point at user k is

$$\rho_{l,k}^r(\mathbf{r}_k(s)) = x_k(s)\sin\theta_{l,k}^r\cos\phi_{l,k}^r + y_k(s)\cos\theta_{l,k}^r, \tag{6}$$

where $(\theta^r_{l,k}, \phi^r_{l,k})$ denote the elevation and azimuth AoAs for the l-th receive paths between the BS and user k. We assume that there are a total of L^t_k AoDs and L^r_k AoAs in the downlink channel matrix between the BS and user k. Consequently, the field-response vector aggregating all AoDs related to user k and the m-th FA at the BS and all AoAs at the user k can be expressed as

$$\mathbf{f}_{k}(\mathbf{t}_{m}(s)) = \left[e^{j\frac{2\pi}{\lambda}\rho_{1,k}^{t}(\mathbf{t}_{m}(s))}, \cdots, e^{j\frac{2\pi}{\lambda}\rho_{L_{k},k}^{t}(\mathbf{t}_{m}(s))} \right]^{T},$$

$$\mathbf{g}_{k}(\mathbf{r}_{k}(s)) = \left[e^{j\frac{2\pi}{\lambda}\rho_{1,k}^{r}(\mathbf{r}_{k}(s))}, \cdots, e^{j\frac{2\pi}{\lambda}\rho_{L_{k},k}^{r}(\mathbf{r}_{k}(s))} \right]^{T}.$$
(7)

Thus, the downlink communication channel vector from the BS to user k, which is associated with the antenna position vectors, is given by

$$\mathbf{h}_{k}(\mathbf{t}(s), \mathbf{r}_{k}(s)) = \mathbf{F}_{k}^{H}(\mathbf{t}(s)) \mathbf{\Sigma}_{k} \mathbf{g}_{k}(\mathbf{r}_{k}(s)), \tag{8}$$

where $\mathbf{F}_k(\mathbf{t}(s)) \triangleq (\mathbf{f}_k(\mathbf{t}_1(s)), \cdots, \mathbf{f}_k(\mathbf{t}_M(s))) \in \mathbb{C}^{L_k^t \times M}$ signifies the field-response matrix at the BS, while $\mathbf{\Sigma}_k \in \mathbb{C}^{L_k^t \times L_k^r}$ indicates the path-response matrix. This path-response matrix encompasses all multi-path responses between every possible AoA and AoD.

B. Problem Formulation

Our goal is to maximize the trajectory-aware sum rate by jointly designing the transmit beamformer and the antenna trajectory, which is subject to the minimum inter-FA distance, FA speed, and the transmit power constraints. Let $\mathbf{W} \triangleq \{\mathbf{W}(1), \mathbf{W}(2), \cdots, \mathbf{W}(S)\}$, $\mathbf{t} \triangleq \{\mathbf{t}(1), \mathbf{t}(2), \cdots, \mathbf{t}(S)\}$, and $\mathbf{r} \triangleq \{\mathbf{r}(1), \mathbf{r}(2), \cdots, \mathbf{r}(S)\}$, this optimization problem can be formulated as

$$\max_{\mathbf{W}, \mathbf{t}, \mathbf{r}} \quad \sum_{s=1}^{S} \sum_{k=1}^{K} \alpha_k \log(1 + \gamma_k(s))$$
 (9a)

s. t.
$$\sum_{k=1}^{K} \|\mathbf{w}_k(s)\|^2 \le P_{\max}, \quad \forall s$$
 (9b)

$$\|\mathbf{t}_i(s) - \mathbf{t}_j(s)\| \ge D, \forall i \ne j, \forall s$$
 (9c)

$$\|\mathbf{t}_m(s) - \mathbf{t}_m(s-1)\| \le V_{\max}^t \tau, \forall m, \forall s,$$
 (9d)

$$\|\mathbf{r}_k(s) - \mathbf{r}_k(s-1)\| \le V_{\max}^r \tau, \forall k, \forall s,$$
 (9e)

$$\mathbf{t}_m(s) \in \mathcal{C}^t, \quad \mathbf{r}_k(s) \in \mathcal{C}_k^r, \quad \forall s,$$
 (9f)

where all weights should satisfy $\alpha_k \geq 0, \forall k$ and $\sum_k \alpha_k = 1$; P_{\max} is the maximum transmit power budget at each time slot. To simplify the original weighted sum rate maximization problem, we employ a linear receive beamforming strategy, where the estimated signal is expressed as $\hat{s}_k(s) = u_k(s)^* y_k(s), \forall k$, and $\mathbf{u}(s) \triangleq (u_1(s), \cdots, u_K(s))^T \in \mathbb{C}^{K \times 1}$ represents the receive beamformer in the s-th time slot. We assume that $s_k(s)$ and $z_k(s)$ are independent, thus, the derived expected meansquare error (MSE) is given by

$$e_{k}(s) \triangleq \mathbb{E}\left[|\hat{s}_{k}(s) - s_{k}(s)|^{2}\right]$$

$$= 1 + |u_{k}(s)|^{2} (\sigma^{2} + \sum_{j=1}^{K} |\mathbf{h}_{k}^{H}(\mathbf{t}(s), \mathbf{r}_{k}(s))\mathbf{w}_{j}(s)|^{2})$$

$$- 2\operatorname{Re}(u_{k}(s)^{*}\mathbf{h}_{k}^{H}(\mathbf{t}(s), \mathbf{r}_{k}(s))\mathbf{w}_{k}(s)). \tag{10}$$

Inspired by the WMMSE algorithm developed for solving multiuser interference in the conventional communication systems [14], we introduce an auxiliary vector $\mathbf{v}(s) = (v_1(s), v_2(s), \cdots, v_K(s))^T$ and reformulate the FA-enabled WMMSE problem to make it more tractable, i.e.,

$$\min_{\mathbf{W}, \mathbf{t}, \mathbf{r}, \mathbf{u}, \mathbf{v}} \quad \sum_{s=1}^{S} \sum_{k=1}^{K} \alpha_k(v_k(s)e_k(s) - \log(v_k(s)))$$
 (11a)

s. t.
$$\sum_{k=1}^{K} \|\mathbf{w}_k(s)\|^2 \le P_{\max}, \quad \forall s$$
 (11b)

$$\|\mathbf{t}_i(s) - \mathbf{t}_j(s)\| \ge D, \forall i \ne j, \forall s$$
 (11c)

$$\|\mathbf{t}_m(s) - \mathbf{t}_m(s-1)\| \le V_{\max}^t \tau, \forall m, \forall s, \quad (11d)$$

$$\|\mathbf{r}_k(s) - \mathbf{r}_k(s-1)\| \le V_{\max}^r \tau, \forall k, \forall s,$$
 (11e)

$$\mathbf{t}_m(s) \in \mathcal{C}^t, \quad \mathbf{r}_k(s) \in \mathcal{C}_k^r, \quad \forall s,$$
 (11f)

$$\mathbf{v}(s) \ge \mathbf{0}, \quad \forall s.$$
 (11g)

III. BCD METHOD FOR FA TRAJECTORY OPTIMIZATION

The BCD method first decomposes the optimization variables into multiple blocks, and then optimizes one block at a time while keeping the other blocks fixed in each iteration.

A. Transceiver Beamformer Design for Each Time Slot

We first examine the optimization of the beamformer W and the associated variables u and v, assuming FA trajectories t and r fixed. As a result, the transmit beamformer design problem for the s-th time slot is reduced to

$$\min_{\mathbf{W}(s), \mathbf{u}(s), \mathbf{v}(s)} \quad \sum_{k=1}^{K} \alpha_k(v_k(s)e_k(s) - \log(v_k(s))) \quad (12a)$$

s. t.
$$\sum_{k=1}^{K} \|\mathbf{w}_k(s)\|^2 \le P_{\text{max}},$$
 (12b)

$$\mathbf{v}(s) \ge \mathbf{0}.\tag{12c}$$

This problem can be solved iteratively with a closed-form solution [14, Table I]. Specifically, the update of $u_k(s)$, $v_k(s)$, and $\mathbf{w}_k(s)$ are, respectively, given by

$$u_k(s) = \left(\sum_{i=1}^K |\mathbf{h}_k(\mathbf{t}(s), \mathbf{r}_k(s))^H \mathbf{w}_i(s)|^2 + \sigma^2\right)^{-1}$$
$$\mathbf{h}_k(\mathbf{t}(s), \mathbf{r}_k(s))^H \mathbf{w}_k(s), \tag{13a}$$

$$v_k(s) = \left(1 - u_k(s)^* \mathbf{h}_k(\mathbf{t}(s), \mathbf{r}_k(s))^H \mathbf{w}_k(s)\right)^{-1}, \quad (13b)$$

$$\mathbf{w}_k(s) = \alpha_k u_k(s) v_k(s) \left(\mu \mathbf{I}_M + \sum_{i=1}^K \alpha_i |u_i(s)|^2 v_i(s) \right)$$

$$\mathbf{h}_{i}(\mathbf{t}(s), \mathbf{r}_{k}(s))\mathbf{h}_{i}(\mathbf{t}(s), \mathbf{r}_{k}(s))^{H} \right)^{-1}\mathbf{h}_{k}(\mathbf{t}(s), \mathbf{r}_{k}(s)),$$
(13c)

where $\mu \ge 0$ is the optimal dual variable determined by onedimensional search methods such that the constraint (11b) is satisfied.

B. FA Trajectory Design at BS

To streamline computational complexity, we adopt an alternating optimization framework for designing FA configurations. Specifically, when fixing the variables \mathbf{W} , \mathbf{t}_j for all $j \neq m$, and \mathbf{r} , the original optimization problem for determining the m-th FA's position at the BS during the s-th time slot can be effectively simplified to

$$\min_{\mathbf{t}_{m}(s)\in\mathcal{C}^{t}} \qquad \sum_{k=1}^{K} \left(\mathbf{f}_{k}^{H}(\mathbf{t}_{m}(s)) \mathbf{A}_{k,m} \mathbf{f}_{k}(\mathbf{t}_{m}(s)) + \operatorname{Re}(\mathbf{b}_{k,m}^{H} \mathbf{f}_{k}(\mathbf{t}_{m}(s))) \right) \tag{14a}$$

s. t.
$$\|\mathbf{t}_m(s) - \mathbf{t}_i(s)\| > D, \forall i \neq m,$$
 (14b)

$$\|\mathbf{t}_m(s) - \mathbf{t}_m(s-1)\| \le V_{\max}^t \tau, \tag{14c}$$

$$\|\mathbf{t}_m(s+1) - \mathbf{t}_m(s)\| \le V_{\max}^t \tau,$$
 (14d)

where the coefficients $\mathbf{A}_{k,m}$ and $\mathbf{b}_{k,m}$ are, respectively, defined as

 $\mathbf{A}_{k,m}$

$$\triangleq \alpha_k v_k(s) |u_k(s)|^2 ||\mathbf{w}_{m,:}(s)||^2 \mathbf{\Sigma}_k \mathbf{g}_k(\mathbf{r}_k(s)) \mathbf{g}_k(\mathbf{r}_k(s))^H \mathbf{\Sigma}_k^H,
\mathbf{b}_{k,m} \triangleq 2\alpha_k v_k(s) \left(|u_k(s)|^2 \sum_{j=1}^K \left(w_{m,j}(s)^* \sum_{n \neq m} w_{n,j}(s) \right) \right)
\mathbf{g}_k(\mathbf{r}_k(s))^H \mathbf{\Sigma}_k^H \mathbf{f}_k(\mathbf{t}_n(s)) - u_k w_{m,k}(s)^* \mathbf{\Sigma}_k \mathbf{g}_k(\mathbf{r}_k(s)).$$
(15)

Subsequently, we develop a systematic approach for updating the antenna position vector through the minorization-maximization (MM) framework [15]. The effectiveness of this iterative optimization paradigm hinges on constructing a surrogate function that systematically addresses both the objective and constraints through carefully designed upper bounds. During the (n)-th iteration, we establish a minorizing approximation for the constraint function by anchoring the

linearization point at the current position estimate $\mathbf{t}_m(s) = \mathbf{t}_m(s)^{(n)}$, leveraging the analytical properties of the Cauchy-Schwarz inequality through the following procedure

$$\|\mathbf{t}_{m}(s) - \mathbf{t}_{j}(s)\| \ge \frac{(\mathbf{t}_{m}(s)^{(n)} - \mathbf{t}_{j}(s))^{T}(\mathbf{t}_{m}(s) - \mathbf{t}_{j}(s))}{\|\mathbf{t}_{m}(s)^{(n)} - \mathbf{t}_{j}(s)\|}.$$
(16)

Concurrently, we formulate a tractable convex surrogate function for the primal objective through a quadratic approximation strategy centered at the current iterate $\mathbf{t}_m(s) = \mathbf{t}_m(s)^{(n)}$

$$\sum_{k=1}^{K} \left(\mathbf{f}_{k}^{H}(\mathbf{t}_{m}(s)) \mathbf{A}_{k,m} \mathbf{f}_{k}(\mathbf{t}_{m}(s)) + \operatorname{Re}(\mathbf{b}_{k,m}^{H} \mathbf{f}_{k}(\mathbf{t}_{m}(s))) \right)$$

$$\stackrel{(a)}{\leq} \sum_{k=1}^{K} \operatorname{Re}(\hat{\mathbf{b}}_{k,m}^{H} \mathbf{f}_{k}(\mathbf{t}_{m}(s))) + \operatorname{const.}$$

$$\stackrel{(b)}{\leq} \sum_{k=1}^{K} \frac{4\pi^{2}}{\lambda^{2}} \|\hat{\mathbf{b}}_{k,m}\|_{1} \|\mathbf{t}_{m}(s)\|^{2} + (\nabla z_{k}(\mathbf{t}_{m}(s)^{(n)}))$$

$$- \frac{8\pi^{2}}{\lambda^{2}} \|\hat{\mathbf{b}}_{k,m}\|_{1} \mathbf{t}_{m}(s)^{(n)})^{T} \mathbf{t}_{m}(s) + \operatorname{const.},$$

where steps (a) and (b) follow from [16, Lemmas 1-2], and

$$\hat{\mathbf{b}}_{k,m} \triangleq 2(\mathbf{A}_{k,m} - \alpha_k v_k |u_k|^2 ||\mathbf{w}_{m,:}||^2 \cdot ||\mathbf{\Sigma}_k \mathbf{g}_k(\mathbf{r}_k)||^2 \mathbf{I}) \mathbf{f}_k(\mathbf{t}_m(s)^{(n)}) + \mathbf{b}_{k,m}, \quad (18) z_k(\mathbf{t}_m) \triangleq \operatorname{Re}(\hat{\mathbf{b}}_{k,m}^H \mathbf{f}_k(\mathbf{t}_m)).$$

Therefore, the antenna position vector $\mathbf{t}_m(s)$ during the s-th time slot is updated as

$$\mathbf{t}_{m}(s)^{(n+1)} = \underset{\mathbf{t}_{m}(s) \in \mathcal{C}^{t}}{\operatorname{argmin}} \sum_{k=1}^{K} \left(\frac{4\pi^{2}}{\lambda^{2}} \| \hat{\mathbf{b}}_{k,m} \|_{1} \| \mathbf{t}_{m}(s) \|^{2} \right. \\ + \left. \left(\nabla z_{k} (\mathbf{t}_{m}(s)^{(n)}) - \frac{8\pi^{2}}{\lambda^{2}} \| \hat{\mathbf{b}}_{k,m} \|_{1} \mathbf{t}_{m}(s)^{(n)} \right)^{T} \mathbf{t}_{m}(s) \right)$$

$$\text{s. t. } \frac{(\mathbf{t}_{m}(s)^{(n)} - \mathbf{t}_{j}(s))^{T} (\mathbf{t}_{m}(s) - \mathbf{t}_{j}(s))}{\| \mathbf{t}_{m}(s)^{(n)} - \mathbf{t}_{j}(s) \|} \ge D,$$

$$(19a)$$

$$\forall j \neq m, \quad (19b)$$

$$\|\mathbf{t}_m(s) - \mathbf{t}_m(s-1)\| \le V_{\max}^t \tau, \quad (19c)$$

$$\|\mathbf{t}_m(s) - \mathbf{t}_m(s)\| \le V_{\max}, \tag{196}$$

$$\|\mathbf{t}_m(s+1) - \mathbf{t}_m(s)\| \le V_{\max}^t \tau, \tag{19d}$$

which can be efficiently solved by fmincon.

C. FA Trajectory Design at Users

Given fixed parameters W, u, v, and t, the structural independence of individual \mathbf{r}_k , $\forall k$ in the WMMSE formulation (11) admits parallel computation across user indices. This inherent separability in the optimization landscape enables the original FA configuration challenge at the k-th user to condense into the following reduced-dimensional subproblem

$$\min_{\mathbf{r}_{k}(s) \in \mathcal{C}_{k}^{r}} \quad \mathbf{g}_{k}^{H}(\mathbf{r}_{k}(s)) \mathbf{C}_{k} \mathbf{g}_{k}(\mathbf{r}_{k}(s)) + \operatorname{Re}(\mathbf{d}_{k}^{H} \mathbf{g}_{k}(\mathbf{r}_{k}(s)))$$
s. t.
$$\|\mathbf{r}_{k}(s) - \mathbf{r}_{k}(s-1)\| \leq V_{\max}^{r} \tau,$$

$$\|\mathbf{r}_{k}(s+1) - \mathbf{r}_{k}(s)\| \leq V_{\max}^{r} \tau,$$
(20)

where the parameters C_k and d_k are defined as

$$\mathbf{C}_{k} \triangleq \sum_{j=1}^{K} |u_{k}|^{2} \mathbf{\Sigma}_{k}^{H} \mathbf{F}_{k}(\mathbf{t}) \mathbf{w}_{j} \mathbf{w}_{j}^{H} \mathbf{F}_{k}(\mathbf{t})^{H} \mathbf{\Sigma}_{k},$$

$$\mathbf{d}_{k} \triangleq -2u_{k}^{*} \mathbf{\Sigma}_{k}^{H} \mathbf{F}_{k}(\mathbf{t}) \mathbf{w}_{k}.$$
(21)

Building upon the established theoretical framework in (17), we systematically derive a convex relaxation for the primal objective through quadratic surrogate function construction. At the (n)-th algorithmic iteration, this majorization procedure is anchored at the current user-side configuration estimate $\mathbf{r}_k(s) = \mathbf{r}_k(s)^{(n)}$ and we have

$$\mathbf{g}_{k}^{H}(\mathbf{r}_{k}(s))\mathbf{C}_{k}\mathbf{g}_{k}(\mathbf{r}_{k}(s)) + \operatorname{Re}(\mathbf{d}_{k}^{H}\mathbf{g}_{k}(\mathbf{r}_{k}(s)))$$

$$\leq \frac{4\pi^{2}}{\lambda^{2}} \|\hat{\mathbf{d}}_{k}\|_{1} \|\mathbf{r}_{k}(s)\|^{2} + (\nabla z_{k}(\mathbf{r}_{k}(s)^{(n)})$$

$$- \frac{8\pi^{2}}{\lambda^{2}} \|\hat{\mathbf{d}}_{k}\|_{1} \mathbf{r}_{k}(s)^{(n)})^{T} \mathbf{r}_{k}(s) + \operatorname{const.}$$
(22)

where

$$\hat{\mathbf{d}}_k \triangleq 2(\mathbf{C}_k - \sum_{j=1}^K |u_k|^2 ||\mathbf{\Sigma}_k^H \mathbf{F}_k(\mathbf{t}) \mathbf{w}_j||^2 \mathbf{I}) \mathbf{g}_k(\mathbf{r}_k(s)^{(n)}) + \mathbf{d}_k$$

$$z_k(\mathbf{r}_k(s)) \triangleq \operatorname{Re}(\hat{\mathbf{d}}_k^H \mathbf{g}_k(\mathbf{r}_k)).$$

Therefore, the FA position vector $\mathbf{r}_k(s)$ at user k during the s-th time slot is updated as

$$\begin{split} \mathbf{r}_{k}(s)^{(n+1)} &= \underset{\mathbf{r}_{k}(s) \in \mathcal{C}_{k}^{r}}{\operatorname{argmin}} \frac{4\pi^{2}}{\lambda^{2}} \|\hat{\mathbf{d}}_{k}\|_{1} \|\mathbf{r}_{k}(s)\|^{2} \\ &+ (\nabla z_{k}(\mathbf{r}_{k}(s)^{(n)}) - \frac{8\pi^{2}}{\lambda^{2}} \|\hat{\mathbf{d}}_{k}\|_{1} \mathbf{r}_{k}(s)^{(n)})^{T} \mathbf{r}_{k}(s), \quad (24) \\ \text{s. t. } \|\mathbf{r}_{k}(s) - \mathbf{r}_{k}(s-1)\| \leq V_{\max}^{r} \tau, \\ \|\mathbf{r}_{k}(s+1) - \mathbf{r}_{k}(s)\| \leq V_{\max}^{r} \tau. \end{split}$$

$$IV. \ \text{Low-Complexity Design}$$

In practice, employing fmincon or CVX to tackle optimization problems inevitably introduces significant computational overhead. To address this, we propose a low-complexity design approach that limits antenna motion to a specified region, which is called planar motion mode. For clarity, the motion mode in Section III is referred to as the general motion mode.

A. Planar Motion Mode

To reduce computational complexity, on the one hand, to deal with constraint (14b), each FA is restricted to move within a designated planar area and the minimum distance between any two areas is set to D to prevent coupling effects; on the other hand, to deal with constraint (14c)-(14d), the range of antenna motion for each time slot is set within the common internal tangent circle formed by the two circles constituted by its adjacent time slots. Let $\hat{\mathbf{t}}_m(s) \triangleq \frac{\mathbf{t}_m(s-1) + \mathbf{t}_m(s+1)}{2}$ and $\hat{\psi}_m(s) \triangleq V_{\max}^t \tau - \frac{\|\mathbf{t}_m(s-1) - \mathbf{t}_m(s+1)\|}{2}$ represent the center and the radius of the circle, then

$$\|\mathbf{t}_{m}(s) - \hat{\mathbf{t}}_{m}(s)\| < \hat{\psi}_{m}(s).$$
 (25)

The position optimization problem (14) can be recast as

$$\min_{\mathbf{t}_{m}(s)\in\mathcal{C}_{m}^{t}} \sum_{k=1}^{K} \left(\mathbf{f}_{k}^{H}(\mathbf{t}_{m}(s)) \mathbf{A}_{k,m} \mathbf{f}_{k}(\mathbf{t}_{m}(s)) + \operatorname{Re}(\mathbf{b}_{k,m}^{H} \mathbf{f}_{k}(\mathbf{t}_{m}(s))) \right) \qquad (26a)$$
s. t.
$$\|\mathbf{t}_{m}(s) - \hat{\mathbf{t}}_{m}(s)\| \leq \hat{\psi}_{m}(s), \qquad (26b)$$

where C_m^t is the movement area of the m-th FA.

Through the systematic construction of a tight bound surrogate in (17), we establish an iterative refinement framework for the antenna position vector.

$$\begin{aligned} \mathbf{t}_{m}(s)^{(n+1)} &= \underset{\mathbf{t}_{m}(s) \in \mathcal{C}_{m}^{t}}{\operatorname{argmin}} \sum_{k=1}^{K} \left(\frac{4\pi^{2}}{\lambda^{2}} \| \hat{\mathbf{b}}_{k,m} \|_{1} \| \mathbf{t}_{m}(s) \|^{2} \right. \\ &+ \left. \left(\nabla z_{k} (\mathbf{t}_{m}(s)^{(n)}) - \frac{8\pi^{2}}{\lambda^{2}} \| \hat{\mathbf{b}}_{k,m} \|_{1} \mathbf{t}_{m}(s)^{(n)} \right)^{T} \mathbf{t}_{m}(s) \right), \\ \text{s. t. } \| \mathbf{t}_{m}(s) - \hat{\mathbf{t}}_{m}(s) \| \leq \hat{\psi}_{m}(s) \\ &= \Pi_{\mathcal{C}_{m}^{t}} \left(\frac{\mathbf{t}_{m}(s-1) - \sum_{k=1}^{K} \frac{8\pi^{2}}{\lambda^{2}} \| \hat{\mathbf{b}}_{k,m} \|_{1} \hat{\mathbf{t}}_{m}(s)}{\sum_{k=1}^{K} \frac{8\pi^{2}}{\lambda^{2}} \| \hat{\mathbf{b}}_{k,m} \|_{1} + 2\delta^{*}} \right. \\ &+ \frac{\sum_{k=1}^{K} \left(\frac{8\pi^{2}}{\lambda^{2}} \| \hat{\mathbf{b}}_{k,m} \|_{1} \mathbf{t}_{m}(s)^{(n)} - \nabla z_{k} (\mathbf{t}_{m}(s)^{(n)}) \right)}{\sum_{k=1}^{K} \frac{8\pi^{2}}{\lambda^{2}} \| \hat{\mathbf{b}}_{k,m} \|_{1} + 2\delta^{*}} \end{aligned}$$

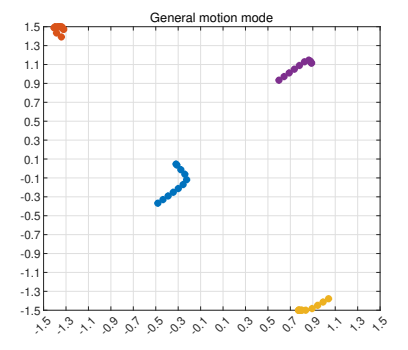
which is a typical convex QP problem, and the closed-form solution is provided in the Appendix. Similarly, we can derive the closed-form solution for the position of the receiving antenna; however, due to space limitations, we omit it.

V. NUMERICAL RESULTS

For quantitative performance evaluation, we establish a multi-antenna base station (BS) configuration with M=4 FAs. The channel path-response matrix elements follow independent and identically distributed (i.i.d.) complex Gaussian distributions. The system parameters are configured with noise power $\sigma^2=15$ dBm and minimum inter-antenna spacing $D=\lambda/2$ to satisfy spatial sampling requirements.

The proposed TFA-RFA scheme is rigorously compared against three baseline configurations: i) Traditional antennas: Conventional static antenna deployment at both ends; ii) TFPA-RFA: BS-side static antennas with user-side position-adjustable FAs within receive regions; iii) TFA-RFPA: User-side fixed antennas with BS-side position-adjustable FAs in transmission regions.

Fig. 1 illustrates two distinct antenna motion paradigms. Notably, optimal positioning requires coordinated nonlinear trajectories rather than direct linear movements, as multiantenna systems necessitate cooperative spatial optimization. Fig. 2 demonstrates the algorithm convergence characteristics, revealing two key observations: (1) negligible performance



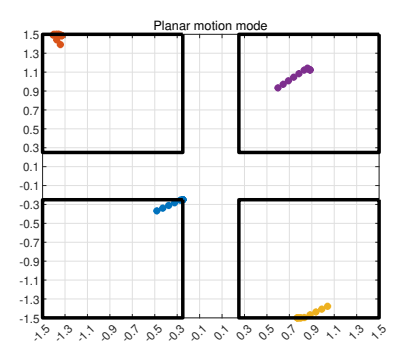


Fig. 1. Antenna trajectory for different motion modes.

variance between motion paradigms in terms of mean sumrate, and (2) significantly accelerated convergence in the lowcomplexity planar motion mode, consistent with theoretical predictions.

Fig. 3 presents the average sum-rate across varying FA configurations, yielding three fundamental conclusions: First, the proposed design achieves consistent performance superiority over all baselines regardless of BS antenna count, with system capacity scaling proportionally to antenna density. Second, increasing position-adjustment degrees of freedom (DoF) produces corresponding performance enhancements, substantiating FA deployment as a capacity-boosting paradigm for next-generation wireless systems. Finally, the planar motion mode attains near-optimal performance while reducing computational complexity, motivating practical implementation of simplified motion-constrained architectures.

VI. CONCLUSION

This paper explored the sum-rate maximization problem through antenna trajectory optimization in FA-enhanced communication systems. To address this challenge, we proposed a BCD-based optimization framework with dual-phase implementation: i) joint beamforming and user association optimization, and ii) constrained FA trajectory design with planar mobility constraints. Particularly, we introduce a planar motion confinement mechanism that restricts each FA's

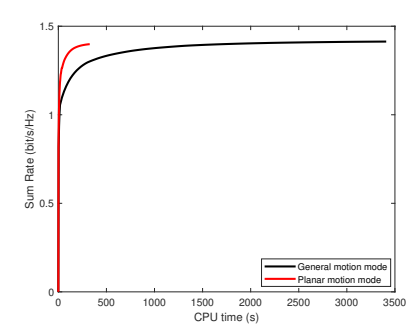


Fig. 2. Convergence performance of the proposed algorithms.

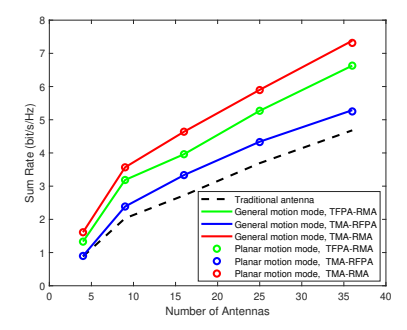


Fig. 3. Evaluation of trajectory-aware sum rate under different M.

movement within predetermined two-dimensional subspaces, effectively reducing computational complexity compared to unconstrained movement scenarios. Simulation results demonstrate that FA technology plays a pivotal role in advancing next-generation reconfigurable wireless architectures.

APPENDIX

We address the solution of (26) via dual decomposition, noting that strong duality is applicable and the duality gap is zero. Let δ denote the multiplier associated to the quadratic constraint $\|\mathbf{t}_m(s) - \hat{\mathbf{t}}_m(s)\|^2 \leq \hat{\psi}_m(s)^2$, the (partial) Lagrangian function for (26) is then formulated as follows:

$$\mathcal{L}(\mathbf{t}_{m}(s), \delta) = \delta(\|\mathbf{t}_{m}(s) - \hat{\mathbf{t}}_{m}(s)\|^{2} - \hat{\psi}_{m}(s)^{2}) + \sum_{k=1}^{K} (\frac{4\pi^{2}}{\lambda^{2}} \|\hat{\mathbf{b}}_{k,m}\|_{1} \|\mathbf{t}_{m}(s)\|^{2} + \bar{\mathbf{b}}_{k,m}^{T} \mathbf{t}_{m}(s)).$$
(28)

where $\bar{\mathbf{b}}_{k,m} = \nabla z_k(\mathbf{t}_m(s)^{(n)}) - \frac{8\pi^2}{\lambda^2} \|\hat{\mathbf{b}}_{k,m}\|_1 \mathbf{t}_m(s)^{(n)}$. The dual function is given by $d(\delta) = \inf_{\mathbf{t}_m(s) \in \mathcal{C}_m^t} \mathcal{L}(\mathbf{t}_m(s), \delta)$. Since $\mathcal{L}(\mathbf{t}_m(s), \delta)$ is convex w.r.t. $\mathbf{t}_m(s)$, we can find the optimal $\mathbf{t}_m(s)$ from the following optimality condition

$$\nabla \mathcal{L}\left(\mathbf{t}_{m}(s), \delta\right) = 2\delta(\mathbf{t}_{m}(s) - \hat{\mathbf{t}}_{m}(s)) + \sum_{k=1}^{K} \left(\frac{8\pi^{2}}{\lambda^{2}} \|\hat{\mathbf{b}}_{k,m}\|_{1} \mathbf{t}_{m}(s) + \bar{\mathbf{b}}_{k,m}\right) = \mathbf{0},$$
(29)

which yields

$$\mathbf{t}_{m}(s) = \hat{\mathbf{t}}_{m}(s) - \frac{\sum_{k=1}^{K} \left(\frac{8\pi^{2}}{\lambda^{2}} \|\hat{\mathbf{b}}_{k,m}\|_{1} \hat{\mathbf{t}}_{m}(s) + \bar{\mathbf{b}}_{k,m}\right)}{\sum_{k=1}^{K} \frac{8\pi^{2}}{\lambda^{2}} \|\hat{\mathbf{b}}_{k,m}\|_{1} + 2\delta}.$$
(30)

Then, $\mathbf{t}_m(s)$ is projected onto the planar area \mathcal{C}_m^t , which leads to the desired (27). $\delta^* \geq 0$ is the multiplier such that $0 \leq \delta^* \perp \|\mathbf{t}_m(s)^{(n+1)} - \mathbf{t}_m(s-1)\| - V_{\max}^r \tau \leq 0$.

REFERENCES

- [1] W. K. New, K. K. Wong, H. Xu, C. Wang, F. R. Ghadi, J. Zhang, J. Rao, R. Murch, P. Ramírez-Espinosa, D. Morales-Jimenez, C.-B. Chae, and K. F. Tong, "A tutorial on fluid antenna system for 6G networks: Encompassing communication theory, optimization methods and hardware designs," *IEEE Commun. Surv. & Tut.*, DOI: 10.1109/COMST.2024.3498855, 2024.
- [2] K. K. Wong, A. Shojaeifard, K.-F. Tong, and Y. Zhang, "Fluid antenna systems," *IEEE Trans. Wireless Commun.*, vol. 20, no. 3, pp. 1950–1962, Mar. 2021.
- [3] K. K. Wong, A. Shojaeifard, K.-F. Tong, and Y. Zhang, "Performance limits of fluid antenna systems," *IEEE Commun. Lett.*, vol. 24, no. 11, pp. 2469–2472, Nov. 2020.
- [4] X. Chen, B. Feng, Y. Wu, D. W. K. Ng, and R. Schober, "Joint beamforming and antenna movement design for moveable antenna systems based on statistical CSI," in *Proc. IEEE Global Communications Conference (Globecom)*, Kuala Lumpur, Malaysia, Dec. 2023, pp. 1–6.
- [5] Y. Ye, L. You, J. Wang, H. Xu, K.-K. Wong, and X. Gao, "Fluid antenna-assisted MIMO transmission exploiting statistical CSI," arXiv:2312.07895, Dec. 2023.
- [6] Z. Cheng, N. Li, J. Zhu, X. She, C. Ouyang, and P. Chen, "Sumrate maximization for fluid antenna enabled multiuser communications," *IEEE Commun. Lett.*, vol. 28, no. 5, pp. 1206–1210, May 2024.
- [7] H. Xu, K.-K. Wong, W. K. New, G. Zhou, R. Murch, C.-B. Chae, Y. Zhu, and S. Jin, "Capacity maximization for FAS-assisted multiple access channels," arXiv:2311.11037, Nov. 2023.
- [8] H. Qin, W. Chen, Z. Li, Q. Wu, N. Cheng, and F. Chen, "Antenna positioning and beamforming design for fluid-antenna enabled multiuser downlink communications," arXiv:2311.03046, Nov. 2023.
- [9] F. R. Ghadi, K.-K. Wong, F. J. López-Martínez, W. K. New, H. Xu, and C.-B. Chae, "Physical layer security over fluid antenna systems: Secrecy performance analysis," *IEEE Trans. Wireless Commun.*, Early Access, 2024
- [10] C. Wang, G. Li, H. Zhang, K.-K. Wong, Z. Li, and D. W. K. Ng, "Fluid antenna system liberating multiuser MIMO for ISAC via deep reinforcement learning," *IEEE Trans. Wireless Commun.*, vol. 23, no. 9, pp. 10879–10894, Sep. 2024.
- [11] D. Zhang, S. Ye, M. Xiao, K. Wang, M. D. Renzo, and M. Skoglund, "Fluid antenna array enhanced over-the-air computation," *IEEE Wireless Commun. Lett.*, vol. 13, no. 6, pp. 1541–1545, Jun. 2024.
- [12] Y. Zuo, J. Guo, B. Sheng, C. Dai, F. Xiao, and S. Jin, "Fluid antenna array for mobile edge computing," *IEEE Commun. Lett.*, vol. 28, no. 7, pp. 1728–1832, Jul. 2024.
- [13] H. Wang, Y. Shen, K.-F. Tong, and K.-K. Wong, "Continuous electrowetting surface-wave fluid antenna for mobile communications," in *Proc. IEEE Region 10 Conference (TENCON)*, Hong Kong, 2022, pp. 1–3.
- [14] Q. Shi, M. Razaviyayn, Z.-Q. Luo, and C. He, "An iteratively weighted MMSE approach to distributed sum-utility maximization for a MIMO interfering broadcast channel," *IEEE Trans. Signal Process.*, vol. 59, no. 9, pp. 4331–4340, Sep. 2011.
- [15] Y. Sun, P. Badu, and D. P. Palomar, "Majorization-minimization algorithms in signal processing, communications, and machine learning," *IEEE Trans. Signal Process.*, vol. 65, no. 3, pp. 794–816, Feb. 2017.
- [16] B. Feng, Y. Wu, X.-G. Xia, and X. Xiao, "Weighted sum-rate maximization for movable antenna-enhanced wireless networks," *IEEE Wireless Commun. Lett.*, vol. 13, no. 6, pp. 1770–1774, Jun. 2024.